

A Novel Strategy for Smooth Force-Position Switching Control of Micropositioning Piezoelectric Actuators

Navid Fallahinia, Mohammad Zareinejad, Heidar Ali Talebi, Keivan Baghestan, Hamed Ghafarirad

Abstract—Control of the exerted force on objects as well as the position of the actuator during a cell characterization operation has an essential role in achieving an efficient performance. In such operations, any undesired applied force could degrade the efficiency or make damages to the object. A challenging problem associated with application to cell characterization using a piezoelectric actuator is to design a suitable force-position switching control law and also to deal with nonlinear hysteretic behavior of such actuators. The main concern in this operation is to provide a smooth switching transition between position and force control modes. A modified Prandtl-Ishlinskii (PI) operator and its inverse are utilized for both identification and real time compensation of the hysteresis nonlinear behavior. By proposing an appropriate force-position switching control approach, the smooth transition between these two modes is guaranteed. The stability of each controller as well as the switching system is demonstrated analytically. Experimental results depict that the proposed approach achieves precise force-position control within each modes and also the switching remains smooth.

I. INTRODUCTION

Micromanipulation and Microrobotic fields have played an important role in the development of delicate systems for biomedical applications. Among all such medical applications, mechanical characterization of cellular events has been an attractive research area in the last decade. Recent researches in cell biology have revealed the significant role of mechanical properties of a living cell in its functions such as growth and proliferation [1-3]. Most of the micromanipulation and cell characterization tasks are performed by highly trained human operators. However, using an automated system, the involvement of human operators is reduced and the reliability of the operation will be increased. Among all smart actuators which can be used for the purpose of cell characterization, piezoelectric types have been more popular due to their special properties such as high resolution, high natural frequency and fast response [4].

Among the different methods introduced for investigating the mechanical properties of a live cell, a conventional one is to exert static or quasi-static forces to a region on the cell membrane and measure the resultant displacement response [5,6]. To perform a multi-phase cell characterization operation, two different control approaches must be

N. Fallahinia, H. Ghafarirad and K. Baghestan are with the Department of Mechanical Engineering, Amirkabir University of Technology, Tehran, Iran (corresponding author phone: (+98-21)66402044; e-mail: n.falahinia@aut.ac.ir).

H. A. Talebi is with the Department of Electrical Engineering, Amirkabir University of Technology, Tehran, Iran (e-mail: alit@aut.ac.ir).

M.Zareinejad is with the New Technologies Research Center, Amirkabir University of Technology, Tehran, Iran, (e-mail: mzare@aut.ac.ir).

developed for precise positioning in the free motion phase and accurate force exertion in the contact phase. In addition, an appropriate switching criterion is necessary for a smooth transition from the free motion phase to the contact phase, and vice versa.

Dealing with the nonlinear hysteretic behavior of piezoelectric actuators, and designing a suitable control law are the two major challenges associated with the development of a piezoelectric actuator with application to cell characterization. The actuator performance is strongly affected by hysteresis nonlinearity behavior [7]. The hysteresis nonlinearity can be eliminated by modeling and utilizing the inverse model as a compensator. Once the hysteresis nonlinearity is eliminated, the operation performance of the actuator must be guaranteed by an appropriate control design. It is a challenging task to implement position and force control for a piezoelectric micropositioning actuator. In fact, one of the major challenges of these types of controllers is switching between position and force control modes.

The main concern in this application is how to provide a smooth transition between these two modes. Several control structures have been suggested for this purpose. In some studies, impedance control has been utilized to avoid the switching problem [8]. This method requires a very careful selection of the desired position and force trajectories to ensure the desired performance, which makes it rather difficult to implement. Another well-known force control approach works through modeling the compliance of the environment [9]. However, the necessity of an exact dynamic model of the environment with its known impedance parameters is a very conservative assumption. Using an intermediate controller is another method to achieve a smooth transition which is used in [10]. The main difficulty with the extra control mode is its switching stability analysis. Vision-based velocity control for reducing the force overshoot has been proposed in [11]. Implementing this approach would decrease the operation speed which is not appropriate for the purpose of cell characterization.

To this end, the objective of this paper is to propose a robust position-force control strategy for piezoelectric actuators with the capability of smoothly switching between the two modes, which can be used with the application of cell characterization. To achieve this objective, first, a generalized Prandtl-Ishlinskii model and its inverse are utilized for the identification and online feedforward compensation of hysteresis which leads to the elimination of the actuator hysteresis behavior. Then two robust force and position controllers will be designed and then combined using an appropriate switching law in order to provide a smooth transition.

II. GENERAL NONLINEAR DYNAMIC MODELING OF PIEZOELECTRIC ACTUATORS

The equation of motion for the piezoelectric actuator during the free motion can be described as follows:

$$M\ddot{X}(t) + C\dot{X}(t) + KX(t) = H_F(v(t)) \quad (1)$$

Where $X(t)$ and $v(t)$ represent the actuator displacement and input voltage respectively. M , C and K denote mass, damping and stiffness coefficients of the actuator. $H_F(v(t))$ expresses the hysteretic relation between the input voltage and the excitation force.

Considering the fact that piezoelectric actuators possess high natural frequency, in low frequency operations the inertia and damping effects can be neglected. After the identification of the hysteresis mapping between the input voltage and the actuator displacement, $H_X(v(t))$ it is scaled up with a factor K to obtain $H_F(v(t))$. As a result, the dynamic model of the system can be written as follows:

$$M\ddot{X}(t) + C\dot{X}(t) + KX(t) = KH_X(v(t)) \quad (2)$$

The exerted external force F_e would be added to the dynamic model as follows:

$$M\ddot{X}(t) + C\dot{X}(t) + KX(t) = KH_X(v(t)) - F_e \quad (3)$$

The generalized Prandtl-Ishlinskii model is used for both hysteresis identification and compensation [12]. The most important advantage of this model is its simplicity and the fact that its inverse could be calculated analytically. The key idea of an inverse feedforward compensation of hysteresis using PI model is to cascade the inverse hysteresis operator H_x^{-1} with the actual hysteresis. As a result, an identity mapping between the desired actuator output $X_d(t)$ and the actuator response $X(t)$ would be obtained. As shown in Fig. 1, the inverse PI operator H_x^{-1} , uses $X_d(t)$ as an input and transforms it into a control signal $v(t) = H_x^{-1}(X_d)$ which results in $X(t)$ in the hysteretic system that closely tracks $X_d(t)$.

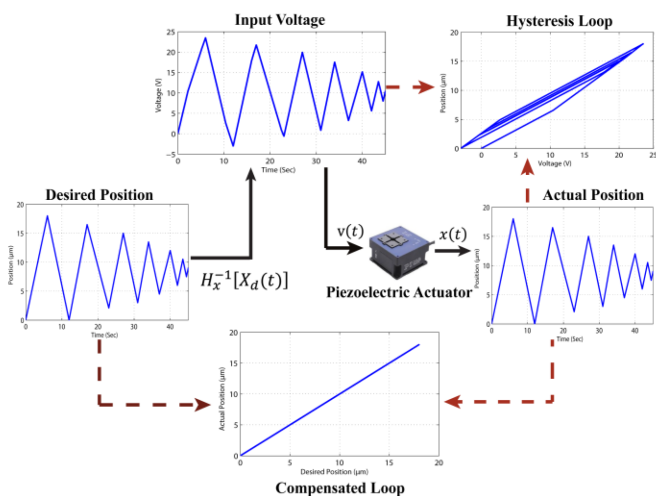


Figure 1. Inverse Feedforward compensation of hysteresis effect.

Utilizing the inverse PI hysteresis model and choosing the input voltage as (4), the dynamic model of the actuator would be transformed to the second-order system as (5).

$$v(t) = H_x^{-1}\left(\frac{1}{K}u(t)\right) \quad (4)$$

$$M\ddot{X}(t) + C\dot{X}(t) + KX(t) = u(t) - F_e \quad (5)$$

Where $u(t)$ is the control input for the inverse PI hysteresis model.

III. ROBUST FORCE-POSITION SWITCHING CONTROL

Because of the parameter uncertainties, hysteresis estimation error and unmodeled dynamics, the general nonlinear dynamic of the piezoelectric micropositioning actuator in contact with the object can be described as below:

$$M\ddot{X}(t) + C\dot{X}(t) + KX(t) = u(t) - F_e + P(t) \quad (6)$$

Where $P(t)$ is the perturbation term. Sliding mode control technique is used for both position and force control which could guarantee the exact performance of the system under the uncertainties.

A. Robust Position Control

The sliding surface for position control and position tracking errors are defined as:

$$\begin{aligned} e(t) &= X_d - X \\ \dot{e}(t) &= \dot{X}_d - \dot{X} \\ S_p(t) &= \dot{e}(t) + \lambda_1 e(t) + \lambda_2 \int_0^t e(t)d\tau \end{aligned} \quad (7)$$

Where S_p is the position sliding surface and λ_1 and λ_2 are positive constants. Substituting the dynamic model (6) to the time derivative of the sliding surface, the control input is obtained as (8).

$$u_p(t) = M\ddot{X}_d + M\lambda_1\dot{e} + M\lambda_2e + C\dot{X}(t) + KX(t) + \eta_1S_p + \eta_2\operatorname{sgn}(S_p) \quad (8)$$

Applying the proposed control input, the closed-loop dynamic error of the system is as follows:

$$M\dot{S}_p + \eta_1S_p + \eta_2\operatorname{sgn}(S_p) + P(t) = 0 \quad (9)$$

Theorem 1: Considering the general dynamic model of the actuator (6) with the perturbation bound $\|P(t)\| \leq \rho$, the robust control input (8) guarantees the asymptotic stability of the closed-loop system.

Proof: The positive definite Lyapunov function candidate for position control $V_p = \frac{1}{2}S_p^2$ would be considered. Substituting the closed-loop dynamic error of the system (9) into the time derivative of the Lyapunov function, \dot{V}_p is achieved as follows:

$$\dot{V}_p = S_p\dot{S}_p \leq M^{-1} \left(-\eta_1S_p^2 - \eta_2|S_p| - S_pP(t) \right) \quad (10)$$

Taking $\eta_2 = \varepsilon + \rho$, with ε denoting an arbitrary positive constant, since $(\varepsilon + \rho)|S_p| \geq S_p P(t)$ it can be derived from (10) that \dot{V}_p is negative semi-definite. The negative semi-definiteness of \dot{V}_p guarantees the boundedness of the Lyapunov function. According to the LaSalle's principle [13], \dot{V}_p tends to zero as $t \rightarrow \infty$ and similarly:

$$t \rightarrow \infty, S_p \rightarrow 0, e \rightarrow 0, \dot{e} \rightarrow 0, x \rightarrow x_d, \dot{x} \rightarrow \dot{x}_d, \quad \square$$

A high gain observer is utilized in order to estimate the velocity state and the signum function in (8) is replaced with the saturation function to reduce the chattering. Finally, the control input (8) would be transformed to:

$$\begin{aligned} u_p(t) = & M\ddot{X}_d + M\lambda_1\dot{e} + M\lambda_2e + C\dot{\hat{X}}(t) + KX(t) \\ & + \eta_1\hat{S}_p + \eta_2 \text{sat}\left(\frac{\hat{S}_p}{\epsilon_1}\right) \end{aligned} \quad (11)$$

Where \hat{X} is the estimated state and ϵ_1 is the thickness of the boundary layer and can be selected to be arbitrarily close to zero.

B. Robust Impedance Force Control

The objective of this section is to accurately control the applied force. In addition, the conservative assumption of known environment should be released. For this purpose impedance control technique is used. The objective of impedance control is to regulate the contact force by achieving a desired impedance behavior between the system and the environment [14]. Suppose that the desired impedance for the system is specified by:

$$M_c\ddot{X}(t) + C_c\dot{X}(t) = F_d - F_e \quad (12)$$

Where M_c and C_c are desired inertia and damping coefficient respectively, and F_d denote the desired applied force. Using the desire impedance of the system, the impedance error would be defined as:

$$\tilde{I}(t) = M_c\ddot{X}(t) + C_c\dot{X}(t) - F_d + F_e \quad (13)$$

The impedance error demonstrates the difference between both sides of the desired impedance, and the desired impedance behavior would be obtained only when $\tilde{I}(t)$ tends to zero. Therefore, the force control sliding surface is defined as:

$$\begin{aligned} S_f(t) = & \frac{1}{M_c} \int_0^t \tilde{I}(\tau) d\tau \\ = & \dot{X} + \frac{C_c}{M_c} + \frac{1}{M_c} \int_0^t (F_e - F_d) d\tau \end{aligned} \quad (14)$$

Substituting the dynamic model (6) to the time derivative of the sliding surface, the control input is obtained as:

$$\begin{aligned} u_F(t) = & -\frac{M}{M_c} (C_c\dot{X} + F_e - F_d) + C\dot{X} \\ & + KX + F_e + \eta_3 \text{sgn}(S_f) \end{aligned} \quad (15)$$

Theorem 2: Considering the described general dynamic model of the actuator (6) with the perturbation bound $\|p(t)\| \leq \rho$, control input (15) guarantees asymptotically stability of closed-loop system.

Proof: Substituting the control input (15) into the system dynamic (6) and adding $\pm M\dot{S}_f$, the closed-loop dynamic error of the system will be as follows:

$$M\dot{S}_f + \eta_3 \text{sgn}(S_f) - P(t) = 0 \quad (16)$$

Substituting the closed-loop dynamic error of the system (16) in the time derivative of the positive definite Lyapunov function candidate $V_f = \frac{1}{2}S_f^2$, \dot{V}_f is achieved as follows:

$$\dot{V}_f = S_f \dot{S}_f = M^{-1}(-\eta_3 |S_f| - S_f P(t)) \quad (17)$$

Taking $\eta_3 = \varepsilon + \rho$, it can be derived from (17) that \dot{V}_f is a negative semi-definite Lyapunov function. Thus, the states of the system can be kept in the region around the sliding surface. This shows the desired impedance characteristic since $\tilde{I} = M_c\dot{S} \approx 0$. \square

As like as the position control approach a high gain observer will be used in order to estimate the velocity state during the contact phase. Thus, the control input (15) would be transformed to:

$$\begin{aligned} u_F(t) = & -\frac{M}{M_c} (C_c\dot{X} + F_e - F_d) + C\dot{X} \\ & + F_e + \eta_3 \text{sat}\left(\frac{\hat{S}_f}{\epsilon_2}\right) \end{aligned} \quad (18)$$

C. Switching Criterion

In cell characterization tasks, the micropositioning actuator initially moves from its initial position toward the object. This movement occurs at a constant velocity in order to prevent large force overshoots when the actuator tip contacts with the object. During this free motion phase the designed robust position controller is employed. As the contact happens, the contact force increases until it exceeds the position to force switching threshold value F_{P2F} . At this time the control system switches to the force control. During the contact phase, the desired contact force F_d is applied by the designed robust impedance controller. After applying the desired force, the actuator tip starts to move away from the object. In the retraction phase as the contact force falls below the force to position switching threshold value F_{F2P} , the controller switches to the position control mode and the actuator tip moves away from the object.

One challenging problem that might occur when the system switches from free motion to contact phase, is multiple switching due to the force overshoot and fluctuations after the impact, which could result in instability. In order to avoid multiple switching, a bound is considered for the threshold values in the switching criterion. The lower bound of the threshold value is F_{P2F} , which is taken as 0.015N. In order to prevent any damage to the object, this value is selected as 10% of the maximum desired force during the contact phase. Moreover, to select this value, the force sensor noise is also considered. The upper bound on the threshold value F_{F2P} must be selected with regard to the maximum force overshoot at the time of the contact, which is 7.9%. Considering the overshoot value, the upper bound for the threshold value is selected as 0.017 N. The switching bounds

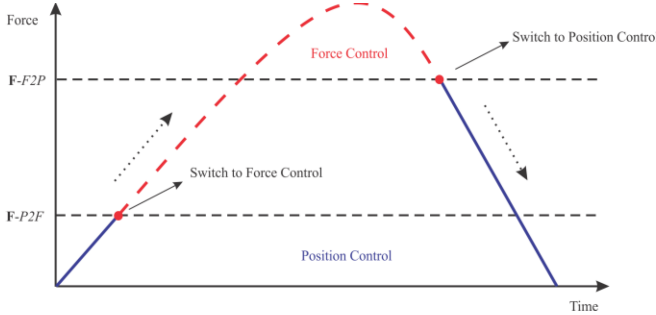


Figure 2. The switching bounds and switching condition.

and the condition for smooth switching between position and force control modes are depicted in Fig. 2.

D. Switching Stability Analysis

In order to deal with stability problem in switching systems there are two different approaches: dwell time and common (or multiple) Lyapunov function [15]. The dwell-time approach is easier to investigate. However, in some cases, it is more conservative in comparison to common and multi-Lyapunov approaches.

Using multiple Lyapunov functions is one the ways for the stability analysis of switching systems. The key idea is based on finding a Lyapunov function which does not increase through the overall time. In a system that switches between two or more asymptotically stable modes, the Lyapunov function for each mode is decreasing. Therefore, asymptotic stability is guaranteed within each mode. However, while the Lyapunov function is decreasing within a specific mode, it is not necessarily decreasing for other modes. As a result, a certain jump in the destination Lyapunov function is observed at the time of switching. This behavior is illustrated in Fig.3 (a).

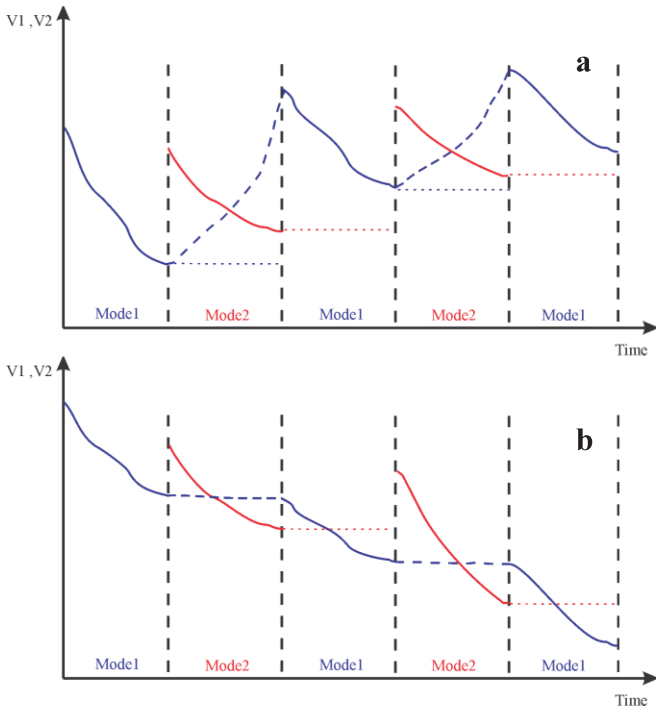


Figure 3. (a) Unstable Lyapunov function (b) stable Lyapunov function with constant value at the second mode.

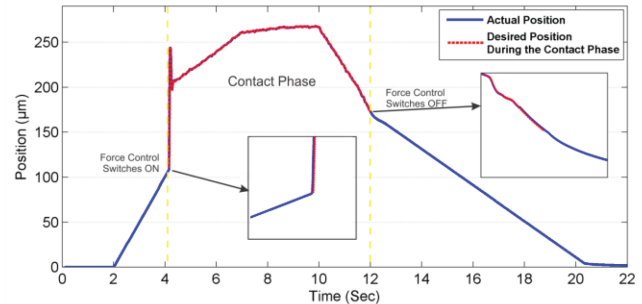


Figure 4. Stability in the switching system utilizing the provided condition.

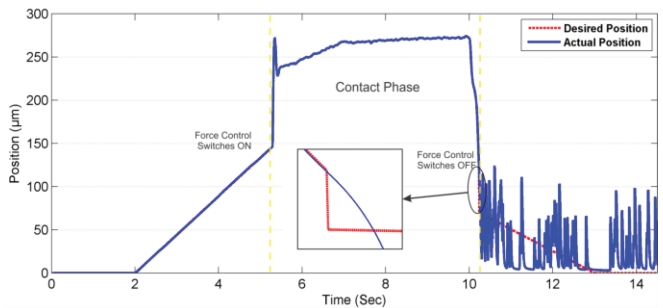


Figure 5. discontinuity in reference position which results in instability.

To achieve stability in this situation, the observed jump in the destination Lyapunov function must be strictly less than the amount of decrease in its previous Lyapunov function in which the total energy of the system is decreasing, resulting in a stable switched system.

For the purpose of this paper, regarding that the switching sequences are not pre-determined and depend on value of contact forces which indicates a state dependent switching, the practical approach is to provide a design that confines the Lyapunov function for the first mode to a constant value when the other modes are active. As shown in Fig. 3 (b), this approach would prevent the total energy of the system from increasing during the switching sequences, which will lead to stability. Recall the Lyapunov functions for position and force control introduced in the previous section. Since the sliding mode approach has been used for designing both controllers, the Lyapunov functions have a similar structure and can be written as follows:

$$V_1(t) = V_{P2F} = \frac{1}{2} S_p^2 \quad (19)$$

$$V_2(t) = V_{F2P} = \frac{1}{2} S_f^2$$

Where S_p is the position sliding surface, which is dependent on the position error and its derivatives. S_f is the force sliding surface and consists of the force error. It was proven in Theorem 1 and Theorem 2 that V_{P2F} and V_{F2P} are decreasing within their own modes of operation.

In order to ensure the stability of the switching system, a condition is put on the desired position trajectory to track the actual position, when the system is in force control mode. This condition would eliminate the position error and its derivatives which restricts V_{P2F} to a constant value within the contact phase. With regard to the fact that there is no restriction on the reference position in contact phase, this

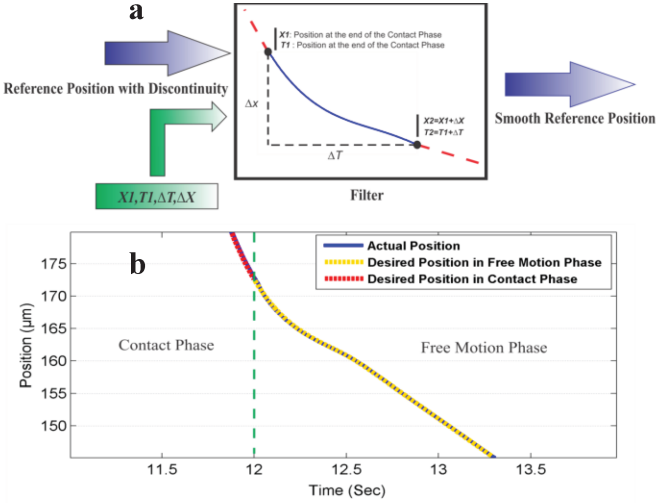


Figure 6. (a) The structure of the filter. (b) Smooth desired position transition from the contact phase to free motion phase.

condition would guarantee the switching stability. Fig. 4 depicts the implementation of this design. It can be seen that the desired position reaches the real position as the force control switches ON and tracks it until the external force falls below the threshold value F_{F2P} .

A problem might arise by implementation of the provided design is a sudden change in the desired position as the system switches back to position control at the end of the contact phase. This change could increase the Lyapunov function which results in instability. This behavior is shown in Fig. 5. To prevent the reference position sudden change, a filter has been proposed in order to provide a smooth desired position. The structure of the filter is depicted in Fig. 6 (a). As can be seen the filter records the reference position and its derivatives at the time of switching as its initial conditions, then designs a spline of the order of three with the time duration of Δt which would provide a smooth desired position transition from the contact phase to retraction phase as shown in Fig. 6(b).

IV. EXPERIMENTAL RESULTS AND DISCUSSION

The proposed control strategy was implemented experimentally. The overall block diagram of the proposed control system is shown in Fig. 7. Moreover, Fig. 8 shows the experimental setup and the micropositioning stage.

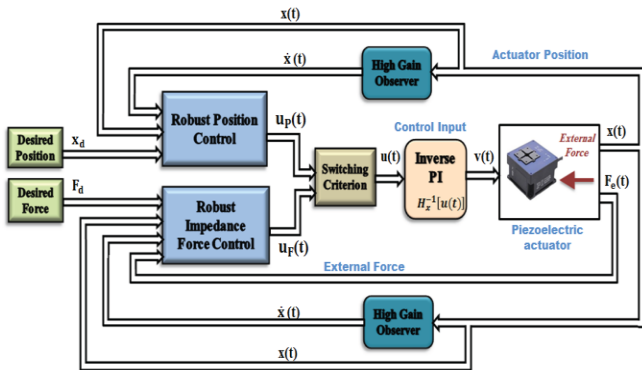


Figure 7. The overall block diagram of the proposed switching force-position control system.

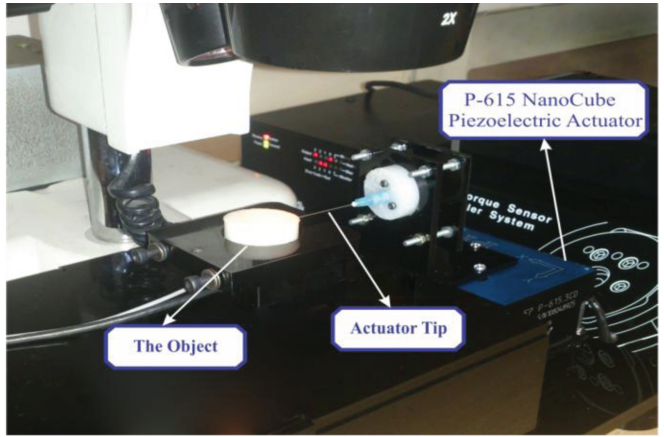


Figure 8. The experimental setup and the micropositioning stage.

The setup contains a P-615 NanoCube piezoelectric actuator with $420 \mu\text{m}$ maximum displacement in X and Y directions. A PCI-1617 Advantech data acquisition and controller board is used for data capturing. Matlab/Simulink software is utilized for implementation of the control approach. A capacitive sensor measures the position of the actuator and an ATI Nano17 force sensor was utilized.

The reference trajectories for the position and force tracking are assigned in Fig. 9(a) and (b) separately. The tracking error is shown in Fig. 9(c) and (d).

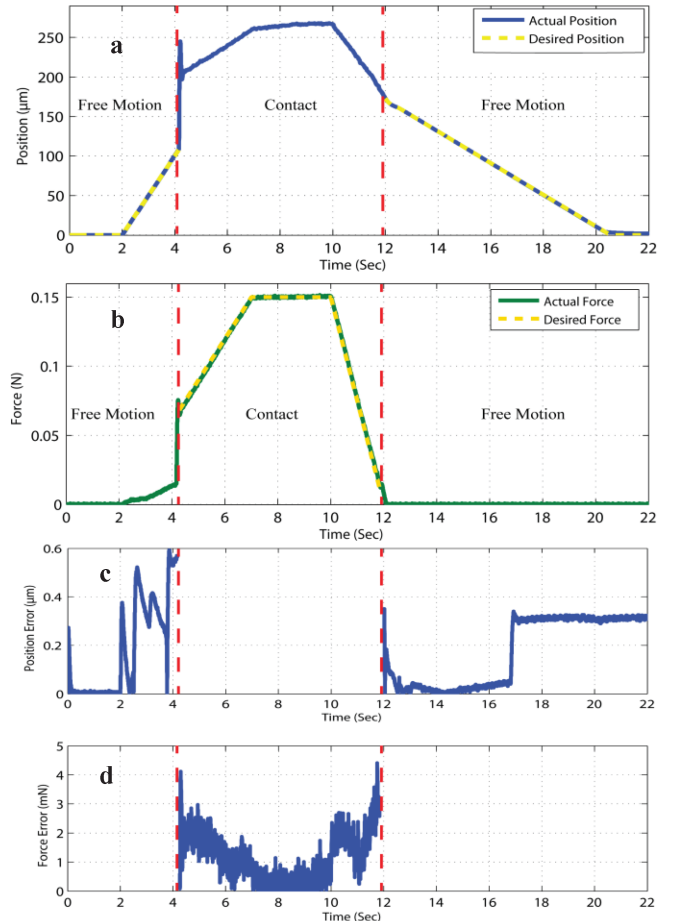


Figure 9. (a),(b) Tracking the desired force and position trajectories in free and contact phases. (c),(d) Tracking errors for force and position references.

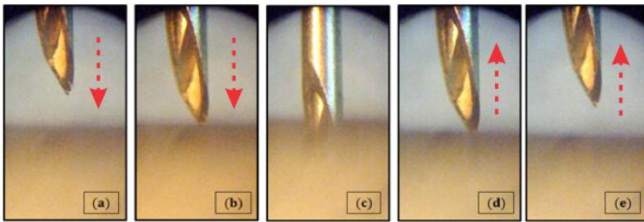


Figure 10. The 5 phases of cell characterization operation

As can be seen in Fig. 9(c) and (d), the maximum absolute errors for the position and force tracking are $0.59 \mu\text{m}$ and 4.48 mN , respectively. During the cell characterization operation the actuator tip first moves toward the object as commanded by the position controller. The tip goes through the environment until the external force arrives at the threshold value F_{P2F} . Then the position control switches to force control to exert a constant desired force of 150 mN on the object for a specified duration of 5 sec . Finally, the applied force reduces to the threshold value F_{F2P} and system is switched over to position control again to take the tip out from the environment at a constant velocity. The 5 phases of cell characterization operation depicts in Fig.10. The satisfactory tracking results demonstrate the robustness property of the developed control scheme under the influence of uncertainties such as unmodeled dynamics and backward hysteresis effect.

Moreover, Fig. 9 depict that a smooth transition between the position and force control has been achieved which indicates the effectiveness of the proposed control strategy in smooth position-force switching control. In Fig. 9 a constant velocity is employed in both penetration and retraction phase, however, different velocities can be achieved in these phases.

V. CONCLUSION

In this paper a robust impedance force-position control approach was designed in order to control the exerted force as well as the position of a piezoelectric micropositioning actuator during a cell characterization process. To achieve this objective an appropriate dynamic modeling of the actuator including nonlinear hysteresis behavior was proposed by using a generalized Prandtl-Ishlinskii model for both hysteresis identification and compensation. Moreover, a sliding mode control algorithm was utilized to ensure the robustness of each controller against the uncertainties such as backward hysteresis effect. In order to provide a smooth transition from free motion phase to contact phase, a robust position control and a robust impedance force control were designed separately for each phase and utilizing a bounded switching criterion, the smooth transition was guaranteed. By using the multiple Lyapunov function method, a condition was provided for the reference position within the contact phase in order to confine the Lyapunov function for the first mode to a constant value when the other mode is active which would guarantee a stable switching. In addition, a filter was designed for a smooth reference position transition from the contact phase to retraction phase to prevent the possible discontinuity in reference position. Finally, the experimental results validate the precise

performance of the force-position control approach as well as its stability.

ACKNOWLEDGMENT

The authors would like to thank the research assistants and staff members of New Technologies Research Center at Amirkabir University of Technology for their kind cooperation.

REFERENCES

- [1] Y.-H. Hsu and W. C. Tang, "A microfabricated piezoelectric transducer platform for mechanical characterization of cellular events," *Smart Materials and Structures*, vol. 18, p. 095014, 2009.
- [2] K. Kim, X. Liu, Y. Zhang, and Y. Sun, "Nanoneutron force-controlled manipulation of biological cells using a monolithic MEMS microgripper with two-axis force feedback," *Journal of Micromechanics and Microengineering*, vol. 18, p. 055013, 2008.
- [3] C. Dagdeviren, Y. Shi, P. Joe, R. Ghaffari, G. Balooch, K. Usgaonkar, et al., "Conformal piezoelectric systems for clinical and experimental characterization of soft tissue biomechanics," *Nature materials*, 2015.
- [4] N. Fallahinia, M. Zarenejad, H. A. Talebi, and H. Ghafarirad, "Robust control of piezoelectric micro positioning actuator using self-sensing method," in *Robotics and Mechatronics (ICROM)*, 2015 3rd RSI International Conference on, 2015, pp. 714-719.
- [5] Y. Shen, U. Wejinya, N. Xi, and C. A. Pomeroy, "Force measurement and mechanical characterization of living drosophila embryos for human medical study," *Proceedings of the Institution of Mechanical Engineers, Part H: Journal of Engineering in Medicine*, vol. 221, pp. 99-112, 2007.
- [6] M. Boukallel, M. Gauthier, M. Dauge, E. Piat, and J. Abadie, "Smart microrobots for mechanical cell characterization and cell convoying," *Biomedical Engineering, IEEE Transactions on*, vol. 54, pp. 1536-1540, 2007.
- [7] H. Ghafarirad, S. M. Rezaei, A. Abdullah, M. Zarenejad, and M. Saadat, "Observer-based sliding mode control with adaptive perturbation estimation for micropositioning actuators," *Precision Engineering*, vol. 35, pp. 271-281, 2011.
- [8] Q. Xu, "Robust Impedance Control of a Compliant Microgripper for High-Speed Position/Force Regulation," *Industrial Electronics, IEEE Transactions on*, vol. 62, pp. 1201-1209, 2015.
- [9] N. Motoi, T. Shimono, R. Kubo, and A. Kawamura, "Task realization by a force-based variable compliance controller for flexible motion control systems," *Industrial Electronics, IEEE Transactions on*, vol. 61, pp. 1009-1021, 2014.
- [10] T. Takahashi, T. Tsuboi, T. Kishida, Y. Kawanami, S. Shimizu, M. Iribe, et al., "Adaptive grasping by multi fingered hand with tactile sensor based on robust force and position control," in *Robotics and Automation, 2008. ICRA 2008. IEEE International Conference on*, 2008, pp. 264-271.
- [11] O. Alkiomaki, V. Kyrki, H. Kalviainen, Y. Liu, and H. Handroos, "Smooth transition from motion to force control in robotic manipulation using vision," in *Control, Automation, Robotics and Vision, 2006. ICARCV'06. 9th International Conference on*, 2006, pp. 1-6.
- [12] W. T. Ang, P. K. Khosla, and C. N. Riviere, "Feedforward controller with inverse rate-dependent model for piezoelectric actuators in trajectory-tracking applications," *Mechatronics, IEEE/ASME Transactions on*, vol. 12, pp. 134-142, 2007.
- [13] H. K. Khalil and J. Grizzle, *Nonlinear systems* vol. 3: Prentice hall New Jersey, 1996.
- [14] S. Jung, T. C. Hsia, and R. G. Bonitz, "Force tracking impedance control of robot manipulators under unknown environment," *Control Systems Technology, IEEE Transactions on*, vol. 12, pp. 474-483, 2004.
- [15] D. Liberzon, *Switching in systems and control*: Springer Science & Business Media, 2012.